SCALING THE VERTICAL STRUCTURE OF SEA BREEZES REVISITED

D. G. STEYN
Atmospheric Science Programme, Department of Earth and Ocean Sciences, The University of British Columbia, Vancouver, B.C. Canada

(Received in final form 8 July 2002)

Abstract. The sea-breeze scaling of Steyn is extended by incorporating data from two additional locations. This is done primarily to remove concerns that the original scaling laws contain features specific to the Vancouver data upon which they were based. This new analysis also employs the integrated, rather than instantaneous, heat flux proposed by Tijm. The analysis results in well-defined scaling laws for all three locations, and include explicit latitude dependence, which was not possible in the earlier study. The integrated heat flux reveals systematic diurnal behaviour that is shown to result in a separate scaling law for diurnal evolution of sea breezes at a single location.

Keywords: Scaling laws, Sea breeze.

1. Introduction

Steyn (1998) presented a scaling scheme designed to reveal universal scaling laws and velocity profiles for a well developed, steady-state sea breeze. The scaling laws were based on a data set collected in the Vancouver, Canada region. Since those data are from a single location, it remains a possibility that aspects of the scaling laws are related to site specific features such as, topographic influences, climatological land-sea temperature contrasts, surface-layer heat flux regimes and surface roughness. In order to reduce the possibility that such site-specific factors influence the resulting scaling laws, this note broadens the applicability of results by repeating the original scaling analysis using the original data from Vancouver, and data from Eastern Spain and The Netherlands. The objectives are to explore scaling relations without the risk of inadvertently incorporating site specific characteristics. An additional value of the extended data set is that the sites are at latitudes 36, 49 and 52 degrees North, thus allowing latitude dependence of scaling laws to be explored, for at least this range of mid-latitude values.

Tijm et al. (1998) and Tijm (1999) employ the scaling introduced by Steyn (1998), but rather than use instantaneous surface-layer turbulent heat flux values in constructing the scaling laws, they use the daily integrated heat flux. The idea behind this approach is that the sea-breeze circulation is more likely to respond to forcing by cumulative, rather than instantaneous, heat input into the boundary layer. Tijm (1999) integrates heat flux over all hours of the day in which it has

Boundary-Layer Meteorology **107:** 177–188, 2003.

positive (upward) values. In the present analysis, the heat flux is integrated over all times it has positive values, from morning up to the time of the sea-breeze profile measurements. This approach is taken since the sea-breeze flow is likely to respond to cumulative heat input into the lower boundary layer since heating started shortly after sunrise, but not to heating that may occur subsequently.

Following Steyn (1998), the sea-breeze flow structure is governed by four dimensionless parameters (Π_1 to Π_4): $\Pi_1 = g\Delta T^2/T_0NH$, $\Pi_2 = f/\omega$, $\Pi_3 = T_0MN/gH$ and $\Pi_4 = N/\omega$, where M is the surface-layer kinematic momentum flux given by $M = \sqrt{(\overline{u'w'})^2 + (\overline{v'w'})^2}$, H is here the time average, integrated surface-layer kinematic sensible heat flux given by:

$$H = \frac{1}{t_p - t_s} \int_{t_s}^{t_p} \overline{w'T'}\, \mathrm{d}t, \tag{1}$$

where $\overline{w'T'}$ is the instantaneous surface-layer kinematic sensible heat flux, t_s is the time at which this flux first becomes positive, t_p is the time at which sea-breeze measurements are taken, $N = \sqrt{g\Gamma/T_0}$ is the Brunt–Vaisala frequency where Γ is the environmental lapse rate (of potential temperature) of the surrounding atmosphere, ΔT is the land–sea temperature difference, f is the Coriolis parameter and ω is the period of diurnal heating. Other variables are conventionally defined.

Following the usual formalism of dimensional analysis, the objective of this work is to search for dimensionless empirical relations of the form:

$$\frac{\phi_{sb}}{\phi_s} = a\Pi_1^b\Pi_2^c\Pi_3^d\Pi_4^e, \tag{2}$$

where Φ_{sb} is a measured dimensional physical property of the sea breeze (in this case, depth and strength), and ϕ_s is the scale appropriate for that quantity. As pointed out by Steyn (1998), Π_1 and Π_3 are related through Monin–Obukhov scaling, and cannot be treated as independent quantities if the velocity profile is specified. The empirical relations are thus only determined for Π_1, Π_2, and Π_4 dependence.

2. The Data and their Analysis

2.1.1. *Data – Vancouver*

All data from Vancouver employed in Steyn (1998) are used in this study, and analyzed in an identical fashion, except for H, which in this work is used in time integrated form.

2.1.2. *Data – Netherlands*

The Royal Netherlands Meteorological Institute operates a large number of synoptic stations throughout that country (see Figure 2.4 in Tijm, 1999). A subset of those data were analyzed by Tijm (1999) in a study of sea breezes. Data from some

of the stations analyzed in that study are appropriate for inclusion in the present work. Many of these stations are located on the west coast of The Netherlands. Apart from a strip of sand dunes near the coast, the orography is nearly flat up to 50 km inland. At a distance 90 km inland the maximum elevation reaches 106 m. Maximum elevations of 200 m do not occur until 150 km inland. The stations used for this study (see Figure 2.4 in Tijm, 1999) were Valkenburg (station 210, 3 km inland), De Bilt (station 260, 50 km inland) and Cabauw (station 348, 45 km inland).

Profiles of wind speed, wind direction and temperature were measured every six hours by a radiosonde at De Bilt. Measurements at Cabauw were taken by a 1290-MHz vertical wind profiler together with a Radio Acoustic Sounding System (Tijm et al., 1998). This sounder produces hourly averaged vertical profiles of wind speed, wind direction and temperature, extending to a height of a few kilometres. In addition to the sounder, the Cabauw station has a 200-m meteorological tower from which near-surface measurements of wind speed, wind direction, humidity and temperature were taken.

Tijm (1999) characterized a sea-breeze day as meeting the following criteria: The average winds between 0600 and 1000 UTC at the land based stations should be directed offshore; the average winds at stations 330 and 210 (see Figure 2.4 in Tijm, 1999) between 1300 and 1600 UTC should be directed on-shore; the maximum (positive) temperature difference between the air over land and over sea should exceed 5 °C. Out of all of the sea-breeze days identified by Tijm (1999), one (27 April 1996) was selected for this study as it showed a number of wind profiles having well-defined sea breeze and return flow aloft. The two profiles used were 1500 and 1600 UTC. Tijm (1999) describes the synoptic situation on 27 April 1996 as being 'dominated by two areas of high pressure, one over Eastern Europe, the second over the Atlantic Ocean, west of Ireland. This situation resulted in a very flat pressure distribution over The Netherlands. In the resulting weak flow and under clear skies ahead of a cold front, a sea breeze developed with the sea-breeze front well-detectable from the surface observations as well as by satellite. The sea-surface temperature was about 7 °C and the maximum measured surface heat flux was 200 W m^{-2}'.

2.1.3. *Data – BEMA Study – Burriana, Spain*

The main objective of the Burriana segment of the Biogenic Emissions in the Mediterranean Area (BEMA) study was to understand and quantify the influence of biogenic volatile organic compound (VOC) emission on the formation of tropospheric ozone (O_3) in the Burriana area (north of Valencia) on the east coast of Spain (Thunis and Cuvelier, 2000). The study incidentally captured a sequence of observations on days dominated by land-sea breeze circulations, thus producing data well suited to the present analysis. For a detailed map of the BEMA study area, see Figure 1 in Thunis and Cuvelier (2000) and Figure 1 in Anastasio et al. (1999). The study, which took place in June 1997, was conducted by several

European institutes and was funded by the European Commission Joint Research Center (Versino, 1997).

The measurement data were collected by three techniques: aircraft, balloons (tethered and free), and surface stations B, C, D and E (see Figure 1 in Anastasio et al., 1999). The aircraft used was the French ARAT (Atmospheric and Remote Sensing Research Aircraft) belonging to IGN (National Geographic Institute) under INSU's (National Institute for the Sciences of Universe) operational responsibility. The aircraft was a FOKKER 27-MK 700 equipped to acquire mean meteorological parameters (wind, T, H, solar radiation) mean physical and chemical parameters (aerosols and ozone) and turbulent parameters enabling the calculation of latent heat, sensible heat, momentum and ozone fluxes (Anastasio, 1999). The four ground stations measured biogenic VOC emissions from local vegetation, the daily changes in O_3 concentration and surface layer turbulent fluxes. The tethered and free balloons measured vertical profiles of wind speed, wind direction, moisture and temperature.

From an analysis of wind direction, temperature and profile data, 11 June and 13 June 1997 were selected for this study. The criteria for their selection were: wind be directed offshore (west-north-westerly) during the morning, and on-shore during the afternoon (east-south-easterly); the maximum land-sea temperature difference be greater than 5 °C, and the profile show a well-defined sea breeze and return flow aloft. The stations used on these days were C, D and Col. (see Figure 1 in Thunis et al., 1998). The synoptic situation on 11 June was characterized by a high-pressure system over the west central Atlantic affecting much of the Iberian Peninsula. This resulted in a weak pressure distribution over southern Spain. A weak low, centered approximately 600 km off the west coast of France, affected the rest of Western Europe. From visible satellite imagery, most of southern Spain was under clear skies with cloudier conditions to the north, which were associated with the low. The same high-pressure system affected southern Spain on the 13 June, but this time the low was centered over the southern portion of the North Sea.

2.2. Ancillary data

2.2.1. *Surface-Layer Turbulent Sensible Heat Flux*

During the BEMA campaign, surface-layer sensible heat flux was measured at stations C and D as 15-min averages. During the Netherlands study, surface-layer sensible heat flux was measured as hourly averages at Cabauw. Steyn (1998) used the instantaneous interpolated value of surface-layer sensible heat flux at the profile start time. This technique has been altered so that the integrated diurnal sensible heat flux from sunrise to the profile start time is used instead of an instantaneous value. The integrals were performed using simple quadrature.

2.2.2. *Land–Sea Temperature Difference*
T_{sea} (as a sea surface temperature) was measured at the Columbretes station in the Balearic Sea (see Figure 1 in Thunis and Cuvelier 2000) during BEMA and in the North Sea near the west coast of The Netherlands during the Netherlands study. The definition of T_{land} employed by Steyn (1998) has been used in this paper. Hourly screen height measurements of T_{land} were taken at Cabauw in the Netherlands. T_{land} was measured every 15 min at the Onda station during the BEMA study.

2.2.3. *Environmental Lapse Rate of Potential Temperature*
The method used for extracting the lapse rates from the Netherlands and BEMA profiles can be found in Steyn (1998).

2.2.4. *Base State Potential Temperature and Period of Diurnal Heating*
The base state potential temperature is taken as the vertically averaged thermal internal boundary-layer temperature extracted from the profile data, and the frequency of diurnal heating is $\omega = 2\pi/24\ \text{h}^{-1} = 7.272 \times 10^{-5}\ \text{s}^{-1}$.

2.2.5. *Coriolis Parameter*
The Coriolis parameter is defined by $f = 2\omega \sin\phi$, where ϕ is the latitude. For this study, $\phi_{\text{Netherlands}} = 52°$, $\phi_{\text{Vancouver}} = 49°$ and $\phi_{\text{BEMA}} = 36°$.

3. Scaling Laws

Functional forms of the scaling laws for sea-breeze strength and depth represented by Equation (2) must be investigated by empirical analysis. Since the present data are drawn from locations having different latitudes, dependence on $\Pi_2 = f/\omega$ can be investigated, albeit in a way limited by only three latitudes in the range 36° to 52° being represented. This remains a substantial advance on Steyn (1998) in which results were valid only for 49°.

By assuming full similarity of all realizations of the sea-breeze circulation, this analysis assumes that there are no fetch (from the shoreline) dependencies in the circulation, and that the circulation is fully adjusted to the heat accumulated in the boundary layer. This last requirement in effect presumes the easily justifiable assumption that time scales of convection driving the sea breeze are shorter than time scales of the surface-layer diurnal cycle.

3.1. Scaling for all data

Scatter plots show that the scaled sea-breeze depth is unrelated to Π_4, as was found in Steyn (1998) but strongly related to Π_1 and Π_2. Exploratory regression analysis employing non-linear least square fitting procedures shows the best relation between z_{sb}/z_s and Π_1 and Π_2 to be:

$$z_{sb}/z_s = 0.75\Pi_1^{1/3}\Pi_2^{-5/2}, \tag{3}$$

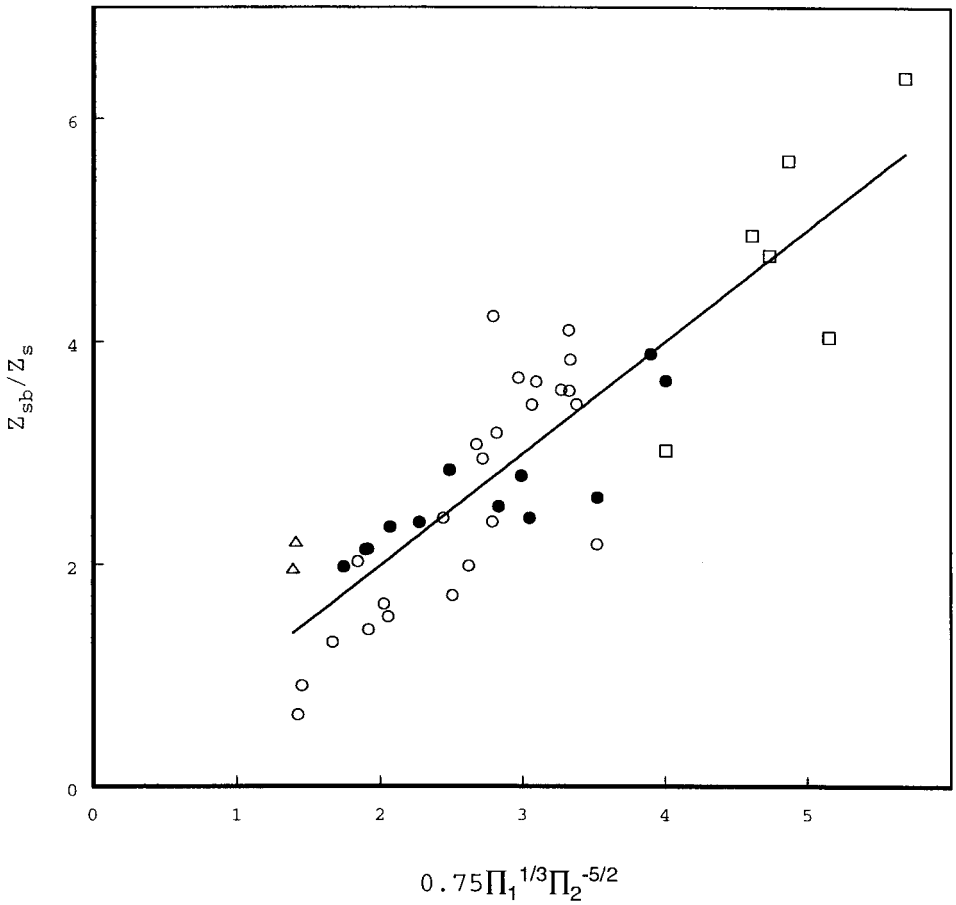

Figure 1. Scatter plot of scaled sea-breeze depth (z_{sb}/z_s) against $0.75\Pi_1^{1/3}\Pi_2^{-5.2}$ where Π_1 and Π_2 are defined in the text. Data points are as follows: ○, Vancouver; □, BEMA; △, Netherlands; ●, Vancouver on 23 August 1985. Solid line is the best fit.

where z_{sb} and z_s (= $H/\omega\Delta T$) are as defined in Steyn (1998). Figure 1 shows the scatter around Equation (3). The standard error of estimate of the coefficient in Equation (3) is 0.02, the linear regression coefficient r^2 is 0.76.

An analysis similar to that for sea-breeze depth shows u_{sb}/u_s to be closely related to Π_1, Π_2 and Π_4, with the best-fit relation being:

$$u_{sb}/u_s = 0.85\Pi_1^{-1/2}\Pi_2^{-9/4}\Pi_4^{1/2}, \tag{4}$$

where u_{sb} and u_s are as defined in Steyn (1998). Figure 2 shows the scatter around Equation (4). The standard error of estimate of the coefficient in Equation (4) is 0.06, and the linear regression coefficient r^2 is 0.63. The relatively large scatters in Figures 1 and 2 match those seen in Steyn (1998), who ascribes them to relatively large errors in wind profile measurements, and the possible influence

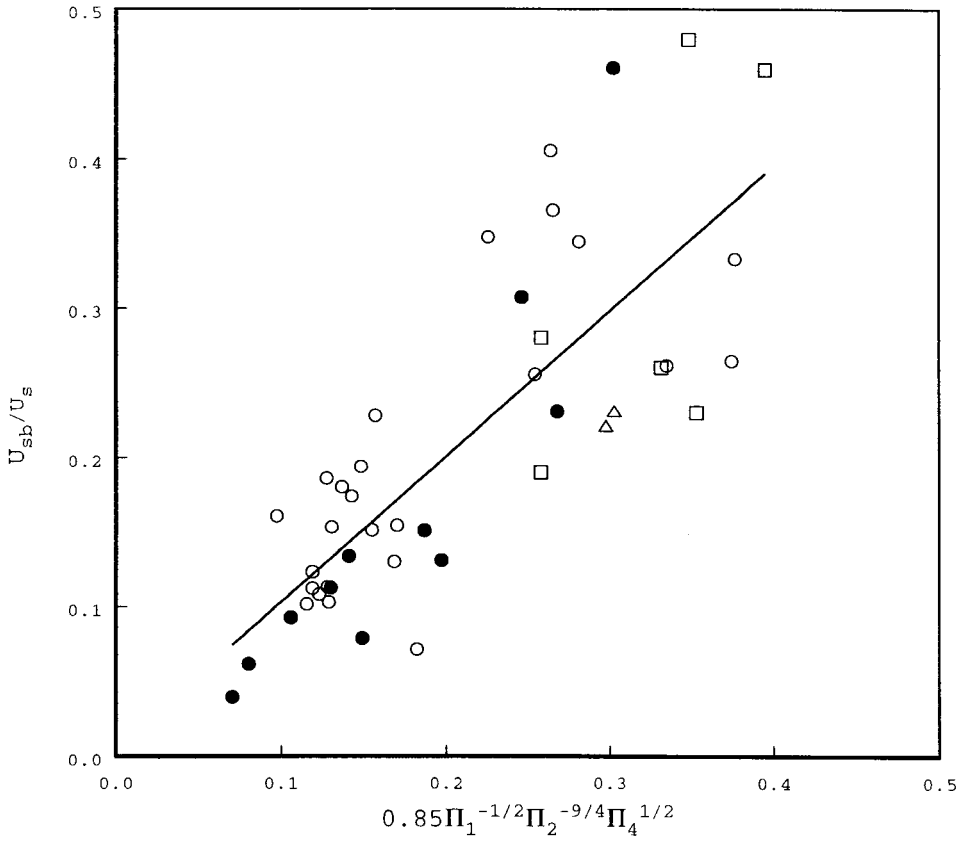

Figure 2. Scatter plot of scaled, vertically averaged sea-breeze strength (u_{sb}/u_s) against $0.85\Pi_1^{-1/2}\Pi_2^{-9/4}\Pi_4^{1/2}$ where Π_1, Π_2 and Π_4 are defined in the text. Data points as follows: ○, Vancouver; □, BEMA; △, Netherlands; ●, Vancouver on 23 August 1985. Solid line is the best fit.

of dependence on variables not included in the scaling analysis. A simple error analysis shows that measurement errors can account for the rather large scatter.

3.2. SCALING FOR DATA TAKEN ON ONE DAY

The Vancouver data set contains a rather remarkable subset of points all taken on August 23, 1985. Eleven profiles taken between 0955 and 1741 Pacific Daylight Time all show a clear sea breeze and return flow. These data are plotted as filled circles in Figures 1 and 2. A careful consideration of this subset of the data provides a more satisfactory explanation (than that based on error analysis alone) of scatter in Figures 1 and 2. Because the heat flux data are incorporated into this analysis as integrals, the variable H is monotonically increasing in time as long as the flux, $w'T'$ is greater than the time average, H. The instantaneous heat flux used in the analysis by Steyn (1998) has a maximum near midday. In the present analysis the

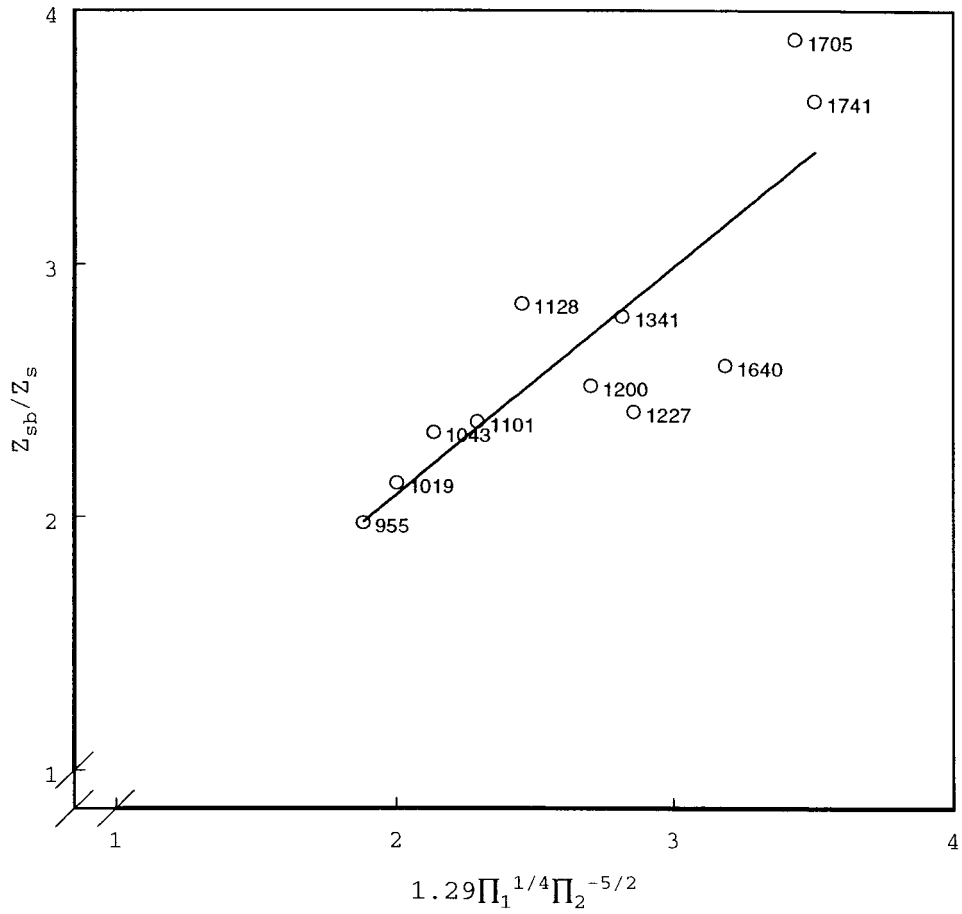

Figure 3. Scatter plot of scaled sea-breeze depth (z_{sb}/z_s) against $1.29\Pi_1^{1/4}\Pi_2^{-5/2}$ where Π_1 and Π_2 are defined in the text. Data are all for Vancouver on 23 August 1985 with time of day in Pacific Daylight Time indicated. Solid line is the best fit.

data points from a single day are sequentially ordered along both axes in Figures 1 and 2. As can be seen in these figures, the points representing this single day have systematic deviations from the best fit line for data from all days (and places). The deviations suggest that the best-fit functions *within* a day may be different from the relation *between* days.

Scatter plots show that the scaled sea-breeze depth for this subset of the data is unrelated to Π_4, but strongly related to Π_1 and Π_2. Exploratory regression analysis employing non-linear least square fitting procedures shows the best relation between z_{sb}/z_s and Π_1 and Π_2 to be:

$$z_{sb}/z_s = 1.29\Pi_1^{1/4}\Pi_2^{-5/2}. \tag{5}$$

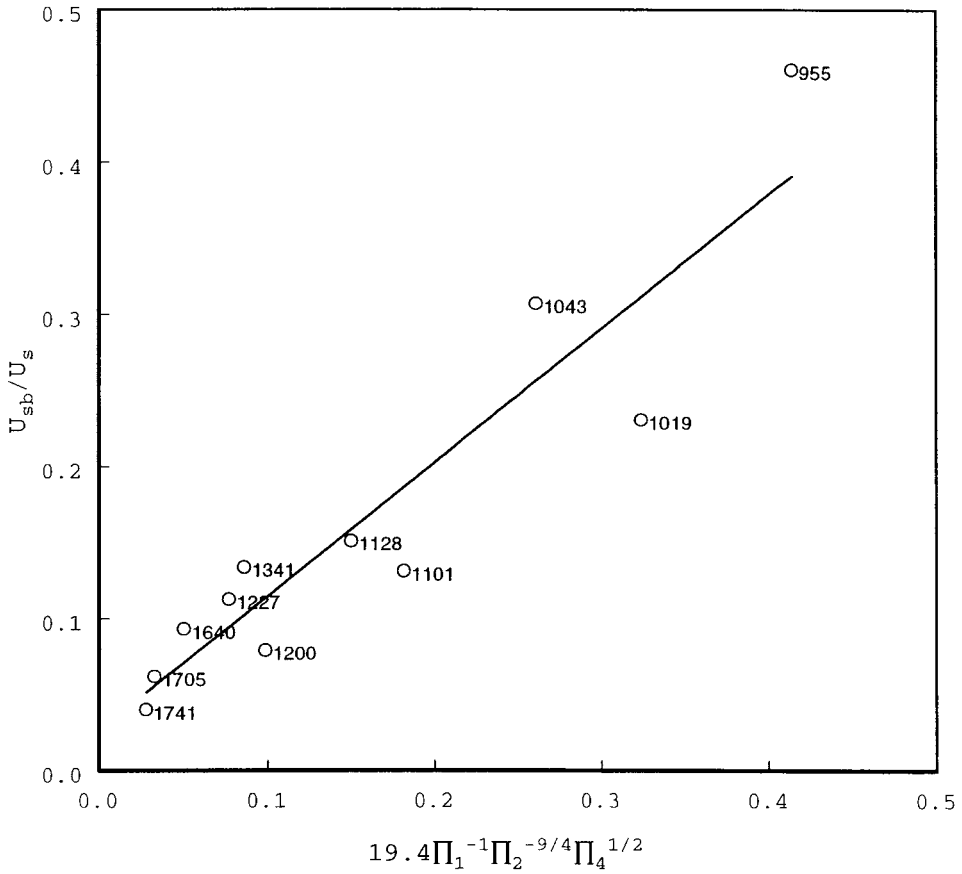

Figure 4. Scatter plot of scaled sea breeze strength (u_{sb}/u_s) against $1.94\Pi_1^{-1}\Pi_2^{-9/4}\Pi_4^{1/2}$ where Π_1, Π_2 and Π_4 are defined in the text. Data are all for Vancouver on 23 August 1985 with time of day in Pacific Daylight Time indicated. Solid line is the best fit.

Figure 3 shows the scatter around Equation (5). The standard error of estimate of the coefficient in Equation (5) is 0.05, the linear regression coefficient r^2 is 0.72.

An analysis similar to that for sea-breeze depth for this subset of the data shows u_{sb}/u_s to be closely related to Π_1, Π_2 and Π_4, with the best-fit relation being:

$$u_{sb}/u_s = 19.4\Pi_1^{-1}\Pi_2^{-9/4}\Pi_4^{1/2}. \tag{6}$$

Figure 4 shows the scatter around Equation (6). The standard error of estimate of the coefficient in Equation (6) is 0.6, and the linear regression coefficient r^2 is 0.87.

There are no other sequences of data on single days in the data set to allow further investigation of this within-day scaling. The meaning of the two scaling laws, one imbedded in the other is quite clear. Equations (5) and (6) represent scalings for the diurnal evolution of the strength and depth of a sea-breeze circulation on a particular day, while Equations (3) and (4) represent scalings for the strength

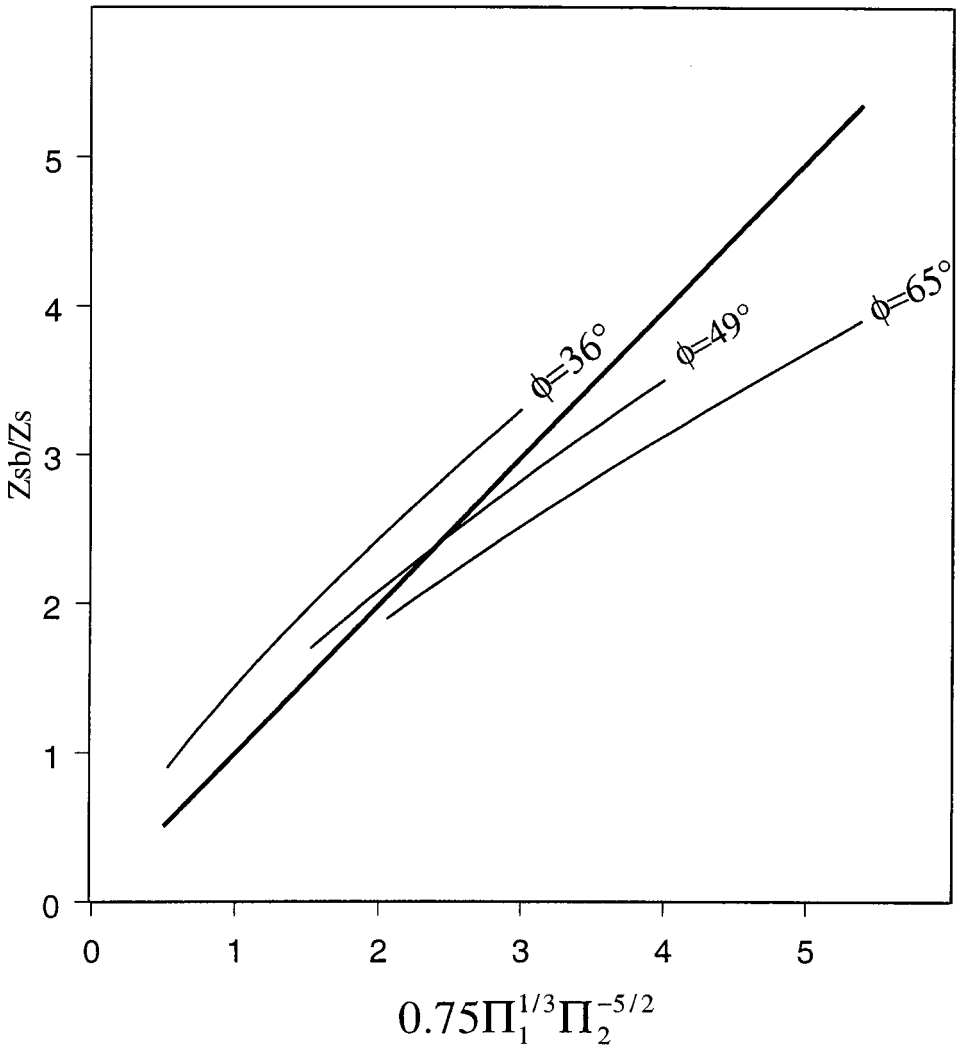

Figure 5. Illustrative plot of scaling laws for diurnal evolution of scaled sea breeze depth (z_{sb}/z_s) at latitudes 36°, 49°, and 65° (fine lines) represented by $1.29\Pi_1^{1/4}\Pi_2^{-5/2}$ in relation to scaling law for all sea breezes (heavy line) represented by $0.75\Pi_1^{1/3}\Pi_2^{-5/2}$.

and depth of all sea breezes. Since the two scaling laws are slightly different, the scatter around Equations (3) and (4) are a consequence of the data points being randomly drawn from a number of days. One may view the within-day scaling laws as each being represented by one of a family of curves, with a large number of these curves making up the total of all possible sea-breeze characteristics on a number of days. If each of these days is represented by only a few points, at random times, the individual daily sequences will not be evident in plots such as Figures 1 and 2. This idea provides a partial explanation for relatively large scatter

of data points around fitted lines in these two figures, and similar figures in Steyn (1998). The relationship between (inter-day and intra-day) scaling laws for sea-breeze depth is easily illustrated by plotting a few examples of Equation (5) in Equation (3) space. This is illustrated in Figure 5 where the three inter-day curves represent latitudes 36°, 49°, and 65°. A similar plot could be constructed for sea-breeze strength, though the illustration is more complication because sea-breeze strength depends on all three independent dimensionless groups.

This phenomenon of imbedded scaling laws is not unknown. Other examples can be found in allometric (power-law) analysis in biological systems. Schreer and Kovacs (1997) in their study of diving capacity in air-breathing vertebrates show that all species obey one scaling law, while particular families or sub-orders obey different, imbedded scaling laws.

3.3. Other scaling issues

The dependence of all scaling laws (Equations (3)–(6)) on Π_2 occur with negative exponents, resulting in infinite depth and strength at the equator where f goes to zero. Data in this study represent a latitude range between 36° and 52°, and thus cannot provide information about the form of scaling laws at low latitudes. Clearly, the scaling laws in Equations (3)–(6) are not applicable at the equator (and surrounding low latitudes), but can be viewed as approximations to the underlying, wide-latitude scaling laws that are valid at a range of mid-latitudes. An obvious (though not the only) modification to these four scaling laws would be to replace $\Pi_2^{-\alpha}$ (where α is either 5/2 for depth or 9/4 for speed) with $(\Pi_2 + \Pi_0)^{-\alpha}$ where Π_0 would have to be determined from data on sea breezes at or near the equator.

4. Conclusions

This analysis of data has extended the sea-breeze scaling laws of Steyn (1998) by including data from two more locations, and by incorporating an integrated, rather than instantaneous heat flux into the analysis. The extension provides strong arguments that the scaling laws are universal since the data now represent conditions in three very different locations, over a range of mid-latitudes.

Incorporating integrated heat fluxes into the analysis following Tijm (1999) has slightly changed the form of resulting power laws, and (because the heat flux now enters as a monotonic variable) has revealed systematic behaviour in data taken on a single day. This has led to the formulation of a set of scaling laws for the diurnal evolution of the sea breeze at one location. It is shown how a family of scaling law curves, each representing the diurnal evolution is embedded within a larger scaling law representing sea breezes at all locations.

An open question that remains to be addressed involves sea-breeze scaling at low latitudes. Since the scaling law representing diurnal evolution is based on

data from one day only, there remains some concern over precision of the empirically determined coefficient and power law exponents. Both questions could be addressed by the application of similar scaling analyses to the output of numerical mesoscale model simulations of sea breezes.

Acknowledgments

I am grateful to Sander Tijm for giving me access to his data, and for discussions about sea-breeze scaling. Philippe Thunis, Kees Cuvelier, Stan Cieslik and Guy Schayes helped in various ways to give me easy access to the BEMA data. Paul Bovis helped tremendously with data analysis, and description of the various data sets. Hiroshi Niino pointed out the difficulty of extending this scaling to the equator. Funding for the research was from grants awarded by the Natural Science and Engineering Research Council of Canada.

References

Anastasio, N., Lopez, A., Attie, J. L., and Durand, P.: 1999, 'Aircraft Measurements during the BEMA Campaign (Burriana, Spain, June 97)', *Phys. Chem. Earth (B)* **25**, 669–672.

Schreer, T. I. and Kovacs, K. M.: 1997, 'Allometry of Diving Capacity in Air-Breathing Vertebrates', *Can. J. Zool.* **75**, 339–358.

Steyn, D.G.: 1998, 'Scaling the Vertical Structure of Sea Breezes', *Boundary-Layer Meteorol.* **86**, 505–524.

Thunis, P. and Cuvelier, C.: 2000, 'Impact of Biogenic Emissions on Ozone Formation in the Mediterranean Area – A BEMA Modeling Study', *Atmos. Environ.* **24**, 467–481.

Thunis, P., Cuvelier, C., and Galmarini, S.: 1998, *BEMA Campaign June 1997 Ozone Evolution at Burriana: Measurements and Modeling*, EUR Report, Luxembourg, Office for Official Publications of the European Commission.

Tijm, A. B. C.: 1999, *Sea-Breeze Studies*, Ph.D. Thesis, University of Utrecht, 183 pp.

Tijm, A. B. C., Holtslag, A. A. M., and Van Delden, A. J.: 1998, 'Observations and Modeling of the Sea-Breeze with the Return Current', *Mon. Wea. Rev.* **127**, 625–640.

Versino, B.: 1997, 'Introduction and Objectives', *Atmos. Environ.* (special issue on the BEMA campaign) **31**(SI), 1–3.